Anal Bioanal Chem (2014) 406:6577–6586
DOI 10.1007/s00216-014-7970-x

RESEARCH PAPER

# Temperature denaturation and aggregation of a multi-domain protein (IgG1) investigated with an array of complementary biophysical methods

**E. Cerasoli · J. Ravi · T. Garfagnini · S. Gnaniah · D. le Pevelen · G. E. Tranter**

Received: 31 March 2014 / Revised: 4 June 2014 / Accepted: 12 June 2014 / Published online: 4 July 2014


**Abstract** Proteins are used as drugs against different pathologies because of their potential specificity of action with fewer side effects. However, their production and successful storage imposes a greater challenge compared to small molecule drugs. Though the determination of protein thermal stability is commonly used to find the optimum storage conditions for biopharmaceuticals, a multi-technique approach should be applied more often when investigating complex systems to understand the structure of the species that contribute to the different transitions, thereby gaining insight about the processes of both unfolding and aggregation. This knowledge is crucial for identifying those conformational changes which are likely to lead to aggregation/degradation allowing a more rational approach to biopharmaceutical production and formulation. This is particularly important in the case of multi-domain proteins, such as IgGs, which can undergo multiple transitions due to independent unfolding of the domains. In this work, we have followed the thermal denaturation of a monoclonal antibody by using different biophysical techniques with complementary strengths, providing an example of how the information gathered suggests a way to intervene to stabilise the wanted conformation (monomeric protein). Indeed, in this particular case, an optimisation of storage conditions based on only thermal stability studies would have led to the stabilisation of an undesired product, a population of low molecular weight oligomers.

**Keywords** Protein aggregation · DSC · FTIR · Circular dichroism · Fluorescence spectroscopy · DLS

Published in the topical collection *Analysis of Biological Therapeutic Agents and Biosimilars* with guest editor Karen Phinney.

**Electronic supplementary material** The online version of this article (doi:10.1007/s00216-014-7970-x) contains supplementary material, which is available to authorized users.

E. Cerasoli (✉) · J. Ravi · T. Garfagnini · G. E. Tranter
Biotechnology Group, National Physical Laboratory, Hampton Road, Teddington, Middlesex TW11 0LW, UK
e-mail: eleonora.cerasoli@npl.co.uk

S. Gnaniah
Materials - Composites / Thermal Analysis, National Physical Laboratory, Hampton Road, Teddington, Middlesex TW11 0LW, UK

D. le Pevelen · G. E. Tranter
Chiralabs Limited, Begbroke Centre for Innovation and Enterprise, Begbroke Science Park, Begbroke Hill, Woodstock Road, Begbroke, Oxfordshire OX5 1PF, UK

*Present Address:*
T. Garfagnini
Institute of Chemistry, The Hebrew University of Jerusalem, Safra Campus, Givat Ram, 91904 Jerusalem, Israel

## Introduction

Monoclonal antibodies (mAbs) represent a class of multi-domain proteins that constitute a relevant fraction of biopharmaceutical products, both on the market or under development. A big effort is put into finding the most suitable set of buffers and additives that preserve the protein in its native conformation, especially at the early stages of development, to minimise failure [1, 2]. In general, proteins are dynamic molecules whose stability in solution can be compromised during production or prolonged storage, resulting in misfolding and impaired quality of the protein product [3–6]. A common outcome of these events is protein aggregation that can affect the stability and activity of biopharmaceutical products and can cause adverse immunogenic reactions [7–10].

Aggregation can follow different pathways. In general, single-domain proteins can interact in their native conformation (N) forming native-like oligomers ($N_i$), or aggregation

can arise from interactions between unfolded proteins (U) resulting in the formation of amorphous aggregates ($U_i$) [11, 12].

$$\begin{array}{ccccc} N & \leftrightarrow & I & \leftrightarrow & U \\ \uparrow\downarrow & & \downarrow & & \downarrow \\ N_i & & I_i & & U_i \end{array}$$

The scenario is further complicated in the case of multi-domain proteins due to the possibility of independent unfolding of the domains and to their different sensitivity to environmental factors, such as pH and buffer composition. This has indeed been observed for IgG whereby the $F_{ab}$ and $F_c$ domains unfold independently [13–17].

In general, an increase in the thermodynamic stability of the protein will decrease the fractional population of partially folded species, which, in the majority of cases, are responsible for aggregation [18]. Though it has been recognised that the temperature denaturation curve ($T_m$) value alone is not always correlated to the product shelf life, these values, optimised under different conditions, are often used to choose the final formulation buffer and excipients for biopharmaceuticals [12, 18–21].

In this regard, differential scanning calorimetry (DSC) appears to be the technique of choice for the determination of the thermodynamic stability of multi-domain proteins being invaluable for gaining an insight into the energetics of the unfolding of the different domains [22, 23]. However, any information on more specific events of protein unfolding such as conformational changes are complex to address by DSC. Indeed, care should be taken when considering the $T_m$ values alone in formulation studies due to the possibility that an increase in $T_m$ reflects the stabilisation of oligomeric species rather than of the monomeric protein. Therefore, attention has to be paid to monitor the structure of the species along the unfolding pathway and in providing information on how these affect protein stability and aggregation.

One approach to achieve a deeper insight and consequently gain a better understanding of the factors underlying protein stability and aggregation is the orthogonal use of different biophysical techniques. This proves to be essential in providing a rationale and time-effective approach to optimise biopharmaceutical production and formulation [4–6, 24–28].

Spectroscopic techniques, such as far-UV circular dichroism (far-UV CD) and Fourier transform infrared (FTIR) spectroscopy, are very useful in gaining insight about the population averaged secondary structure. Their complementarity resides in the fact that the working concentration range is different and that CD is more sensitive to the α-helix content, while FTIR is more sensitive to the amount of β-sheet present. Near-UV CD and fluorescence spectroscopy can be employed in a complementary way to investigate the rigidity and the environment of the aromatic amino acids, disulphide linkages and other chromophoric moieties present. High-performance liquid chromatography-size exclusion chromatography (HPLC-SEC) and dynamic light scattering (DLS) can be used in an orthogonal way to determine the aggregation state of the protein of interest. HPLC-SEC is the most common method used to detect and quantify low molecular weight (LMW) oligomers in a protein solution, but its main drawback is that the sample is not measured at equilibrium. DLS, on the other hand, is a batch technique, where there is no separation of the mixture prior to analysis, and it is sensitive to very small amounts of large aggregates in solution and to sample heterogeneity (Table 1).

## Experimental

The mAb used in this work is an IgG1 formulated at 81 mg/mL in 50 mM citrate, 200 mM NaCl, at pH 5.5 (CBS). All the buffers and chemical used were supplied, at the highest purity available, by Sigma-Aldrich. The protein content was determined using the value of 1.49 for the absorption of a 1-mg/mL solution in a 1-cm cell, on a Lambda-850 UV-Vis spectrophotometer (Perkin Elmer).

*HPLC-SEC* Chromatographic analysis was carried out on a JASCO HPLC with PU2080 Plus pumps equipped with a UV-Vis PDA detector (MD2010 Plus). The samples were separated, at 20 °C, on a TSK-G3000$SW_{XL}$ column (7.8 mm i.d.× 30 cm, 5 μm particle size; Tosoh Bioscience) fitted with a precolumn. The isocratic elution was carried out by injecting 50 μL of a 5-mg/mL IgG solution. The flow rate was set at 0.5 mL/min, and CBS was used as the running buffer to minimise changes in the environment that could affect the aggregate distribution of the IgG [26]. SEC-DLS measurements were carried out using the Malvern Zetasizer Nano equipped with a custom-supplied flow cell and with a special flow-mode operating procedure to allow the measurement of the sample eluting from the column. Correlograms were recorded every 3 s. The column was calibrated using the high molecular weight (HMW) standard kit from Pharmacia according to the instructions provided.

*Far and near-UV circular dichroism spectra* CD spectra were obtained on a J810 spectrophotometer equipped with a PTC423S thermocouple (JASCO). For far-UV CD measurements, the buffer was exchanged to 50 mM phosphate buffer, pH 7, because of the high absorbance of CBS in the far-UV region (ESM Fig. S1). To monitor the unfolding spectra, six accumulations (50 nm/min scan speed, 0.5 nm data pitch, 1 s response time and 1 nm bandwidth) of a 1-mg/mL protein solution, in a 0.01-cm demountable rectangular quartz Cuvette (Hellma) were acquired at different temperatures. The

**Table 1** Summary of the techniques used to detect conformational changes upon thermal denaturation

| Technique | summary | |
|---|---|---|
| Far-UV CD | Changes in secondary structure | Signature characteristic of the overall secondary structure<br>Determination of thermal stability and reversibility<br>Effects of solution conditions and excipients on overall secondary structure<br>Performed under native conditions and in thermodynamic equilibrium |
| FTIR-ATR | | Secondary structure information<br>Sensitive to intermolecular β-sheet aggregation<br>Can be less discriminating than Far-UV CD<br>Performed under native conditions and in thermodynamic equilibrium<br>Good for high-concentration protein solutions<br>Protein binding to ATR crystal can affect result<br>Water gives confounding signals |
| Near-UV CD | Changes in tertiary packing | Detect changes in tertiary structure and environment around aromatic residues<br>Detect changes in disulphide bridges<br>Used as fingerprint |
| Tryptophan fluorescence | | Information about the accessibility of Trp(s) to the solvent |
| DLS | Changes in aggregation state | Sensitive detection of large aggregates and sample heterogeneity<br>Performed under native conditions and in thermodynamic equilibrium<br>Does not resolve low molecular weight oligomers (in batch mode) |
| SEC-UV | | Aggregate amount (quantitative)<br>Molecular weight (qualitative)<br>Sample dilution, filtration and possible interaction with matrix<br>Change of solution conditions with possible changes in equilibrium population<br>High salt concentration may create new aggregates |

temperature was increased with a 2 °C/min gradient (3 min of equilibration time). For Near-UV CD measurements, protein solutions at 1 and 81 mg/mL were used, and the spectra were acquired, respectively, in a 0.5- or 0.01-cm path length rectangular quartz cuvette (Hellma) (six accumulations, 20 nm/min scan speed, 0.2 nm data pitch, 1 s response time and 1 nm bandwidth). During the temperature denaturation experiments, the signal at 273 nm was followed in the 5–75 °C range with a data pitch of 1 °C (360 s of delay time) and a temperature gradient of 1 °C/min. The spectra at different temperatures have been corrected by the thermal expansion.

*FTIR-ATR* Spectra were collected using Tensor-37 FTIR spectrophotometer, Bruker Optics, with a thermostated BioATR II unit and liquid nitrogen-cooled photovoltaic MCT detector. OPUS software was used for data acquisition. So as to ameliorate artefacts that can arise when using an ATR unit, due to interactions of the protein with the unit surface, for the temperature denaturation experiments, the samples were equilibrated for 5 min at the target temperature in a dry block. Small aliquots were then transferred to the ATR unit, equilibrated at the same temperature, for the measurements. The spectra (128 scans, 4 $cm^{-1}$ resolution) were recorded, and the contribution from atmospheric gases was eliminated using an algorithm provided by the OPUS software. The water subtraction was carried out taking into consideration the combination band of water, centred at 2,125 $cm^{-1}$, and by flattening the region from 1,906 to 1,740 $cm^{-1}$ [29]. The FTIR spectra of the gel samples were obtained on the pellet after centrifugation by using the supernatants obtained after centrifugation as blanks to eliminate any contribution from soluble protein still in the solution.

*Fluorescence* Tryptophan fluorescence was measured with a LS55 (Perkin Elmer) at 25 °C using a 1-cm quartz cuvette (Hellma) and 0.1 mg/mL of protein solution. To selectively excite the tryptophan, an excitation wavelength of 295 nm (2.5 nm exCitation slit) was used. The spectra were acquired from 300 to 400 nm (emission slit 6 nm) and subtracted with the corresponding buffer blank. For the temperature denaturation experiments, a temperature gradient of 1 °C/min was

used with a 5-min equilibration time at the target temperature before measurement.

*Dynamic light scattering* DLS measurements were carried out on a Zetasizer Nano, Malvern Instruments. The IgG solutions were at 81 mg/mL or diluted to 1 mg/mL in CBS. No filtration of the sample was carried out before the measurements so as not to affect the aggregate population. The data were analysed using the manufacturer's Dispersion Technology Software, looking at both the cumulant (single exponential—[30]) and multimodal (multi-exponential-Malvern, DTS algorithm) analysis. For the temperature denaturation experiments, the samples were heated with steps of 5 °C between 25 and 65 °C and 1 °C between 65 and 80 °C using the inbuilt Peltier temperature control, with 5 min of equilibration time, and three sub-runs were measured at each temperature. The measurements were carried out in triplicates over different days. Wherever error bars are reported, these are the standard deviation between days (between the averages of the sub-runs on the same day). The onset of the increase in the derived count rate (kcps) was taken as aggregation temperature [31]. Because the sample, at both concentrations tested, aggregates at 73 °C, we have expressed the changes in the different parameters taking 72 °C as the final temperature:

$$\%\text{Total Change} = \frac{(Y_{X^{\circ}\text{C}} - Y_{25^{\circ}\text{C}}) \times 100}{(Y_{72^{\circ}\text{C}} - Y_{25^{\circ}\text{C}})}$$

*Differential scanning calorimetry* The experiments were carried out on a DSCQ2000 instrument from TA Instruments. The samples (duplicate measurements) of the IgG1 at 81 mg/mL in CBS were placed in sealed aluminium crucibles along with the CBS as the reference sample. The heating rate was of 1 °C/min. The data were analysed using the TA Universal Analysis software.

## Results and discussion

*Characterisation of the unstressed IgG* At first, we have characterised the unstressed IgG by measuring its average secondary structure, its tertiary packing and aggregation state.

The far-UV CD spectrum (Electronic Supplementary Material (ESM) Fig. S2, black line), with its negative maximum at ~217–218 nm, indicates intramolecular β-sheets as the most abundant secondary structure, as expected for an IgG. The FTIR-ATR spectrum (ESM Fig. S3) has the typical signature of β-sheet proteins with the amide I second derivative spectrum presenting two main bands, respectively at 1,636 and 1,690 $cm^{-1}$, a shoulder at ~1,672 $cm^{-1}$ likely assigned to turns.

As expected, the near-UV CD has the same shape as other IgG spectra reported elsewhere [26] with bands at a wavelength above 285 nm indicative of Trp residues placed in a particular environment and bands around 265 and 270 nm which could be assigned to Phe and Tyr transitions (ESM Fig. S4). The fluorescence spectrum (ESM Fig. S5) presents two shoulders, one close to 335 nm and the other around 346 nm. This is normal for a multi-tryptophan protein where there are contributions to the spectrum from tryptophans experiencing different protein environments [32]. In this case, the two bands are indicative of the presence of two Trp populations with the one, presenting fluorescence intensity maximum at lower wavelengths, more buried into the protein core.

The HPLC-SEC chromatogram shows the presence of ~2 % aggregates in the unstressed sample (ESM Fig. S6). The hydrodynamic diameter ($d_H$) of the non-stressed IgG was determined by DLS. Overall, the hydrodynamic diameters obtained, with the corresponding values of PdI (0.07), are indicative of mainly monomeric species in solution, which is in agreement with those obtained from HPLC-SEC.

*Structural changes and aggregation upon thermal denaturation* DSC experiments were performed by using the IgG as formulated (81 mg/mL). The thermogram in Fig. 1 shows a transition with $T_m$=76.5 °C and a shoulder at lower temperatures that indicates a process with an onset at around 63 °C. At the end of the scan, the protein was irreversibly aggregated as evident by the formation of an insoluble, gel-like material in the crucible.

The presence of two transitions, previously observed for some other IgGs [13–17], is thought to derive from the independent unfolding of the IgG domains. It is reasonable, therefore, to assign the shoulder to a first, unresolved transition, followed by another transition with a higher $T_m$ and larger experimental enthalpy. Because of the overlap of the two transitions, it was not possible to derive thermodynamic parameters. One possible explanation for the lack of resolution between the two transitions, already observed before for IgGs, could be due to the different sensitivity of the IgG domains toward changes in temperature [15]. Further experiments are necessary to give more insights into the nature of these two transitions.

*Changes in the secondary structure upon thermal denaturation* The far-UV CD spectra show minor changes until 75 °C (ESM Fig. S2). At this temperature, there is an increase in the scattering and the antibody starts to aggregate and precipitates, forming a gel.

The FTIR spectra do not show any major changes in the position of the main peak (1,636 $cm^{-1}$) over the complete temperature range, but minor changes can be observed in two areas of the amide I band: around 1,672 $cm^{-1}$ and around 1,623 $cm^{-1}$ (Fig. 2a). Changes occurring around 1,623 $cm^{-1}$ can be indicative of an increase of the fraction of

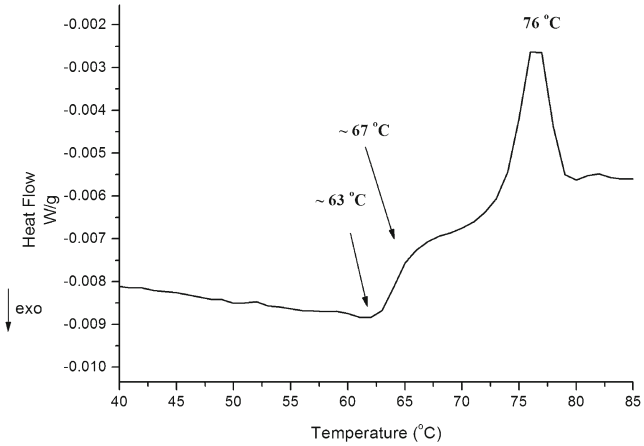


**Fig. 1** DSC thermogram of the IgG (81 mg/mL, CBS). Heating rate 1 °C/min

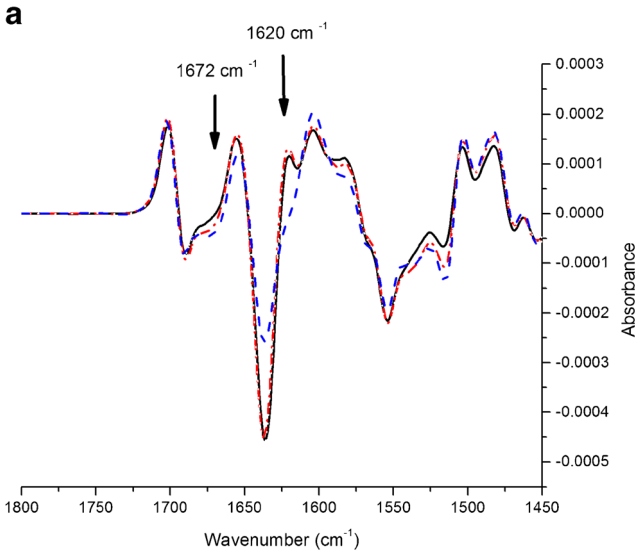


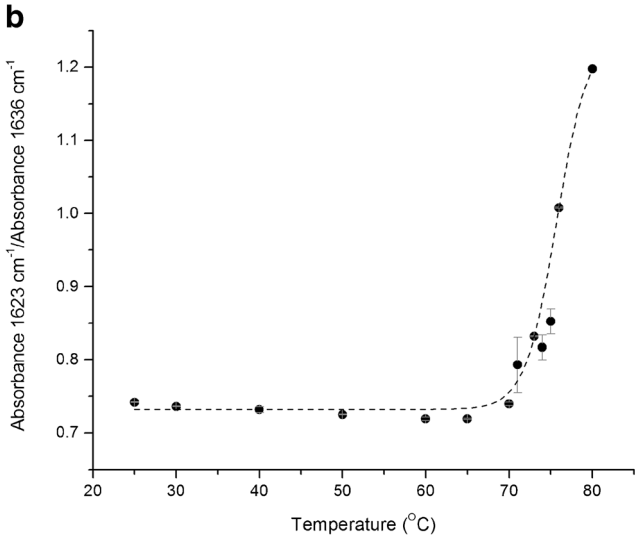


**Fig. 2** **a** Second derivative (Savitzky-Golay 20 point smoothing) of the FTIR spectra acquired at different temperatures of the IgG at 81 mg/mL in CBS. *T*=25 °C (*black line*), *T*=65 °C (*red dashes*) and *T*=75 °C (*blue dashes*). **b** Changes in the ratio of the FTIR absorbance at 1,623 and 1,636 $cm^{-1}$ with temperature. The data points were fitted with a sigmoidal function (Boltzmann) only for explanatory purposes

intermolecular (as opposed to intramolecular) β-sheets. Therefore, we have followed the variation of the ratio between the absorbance at 1,623 and 1,636 $cm^{-1}$ (Fig. 2b). No changes are observed until the onset of the aggregation (72–73 °C).

Both the FTIR and the far-UV CD data suggest that the first transition, observed in the DSC experiment, with an onset temperature around 63 °C does not reflect an unfolding of the secondary structure.

*Changes in the tertiary packing upon thermal denaturation* The near-UV CD is sensitive to small changes in the tertiary packing. The measured near-UV CD of aromatic amino acid residues with freedom of motion, as in our case (Fig. 3a, black line), is typically only of small magnitude compared to that possible when rigidly held. Nonetheless, the denaturation curve (Fig. 3b) and the spectra (Fig. 3a) at different temperatures and the denaturation curve (Fig. 3b) show a decrease of differential absorption measurement CD magnitude at 273 nm after 60 °C. This decrease in signal indicates a probable further loss in the rigidity of the aromatic amino acid environment. The melt was stopped at 74 °C because at this temperature, the sample formed a gel-like aggregate.

The major differences are observed for the bands at 260–270 nm, while the bands at higher wavelengths (>285 nm) are not markedly affected by the increase in temperature.

Signals in the region below 285 nm arise mainly from both Phe (250–270 nm) and Tyr (270–290 nm). Between 25 and 62 °C, there are only minor changes in the tyrosine regions that could be due to the instrumental noise. The spectra at 64 and 65 °C, instead, present visible differences from the spectrum at 25 °C.

In the Phe region (Fig. 3a), the signal decreases, most likely indicating a loss in the rigidity of the environment of this amino acid (unfolding), and this temperature corresponds to the first transition observed in the DSC experiment. Minor changes are also present at $\lambda$>285 nm. In this region, there is a change in the spectrum, but not a decrease in signal intensity, which is consistent with a change in the Trp environment that does not result in a substantial loss of rigidity. The further increase of temperature above 65 °C does not result in any change in the near-UV CD spectrum. After 70 °C, the sample starts to aggregate leading to a concomitant increase in the absorbance (Fig. 3c).

Fluorescence measurements were done at a concentration of 0.1 mg/mL. At this concentration, no visible aggregation is observed at 75 °C (end of the melt). In the case of a multi-tryptophan protein such as an IgG, Trp populations in different environments will contribute differently to the spectrum, and therefore the intensity, upon unfolding, can either decrease or increase. In our case, the intensity for the

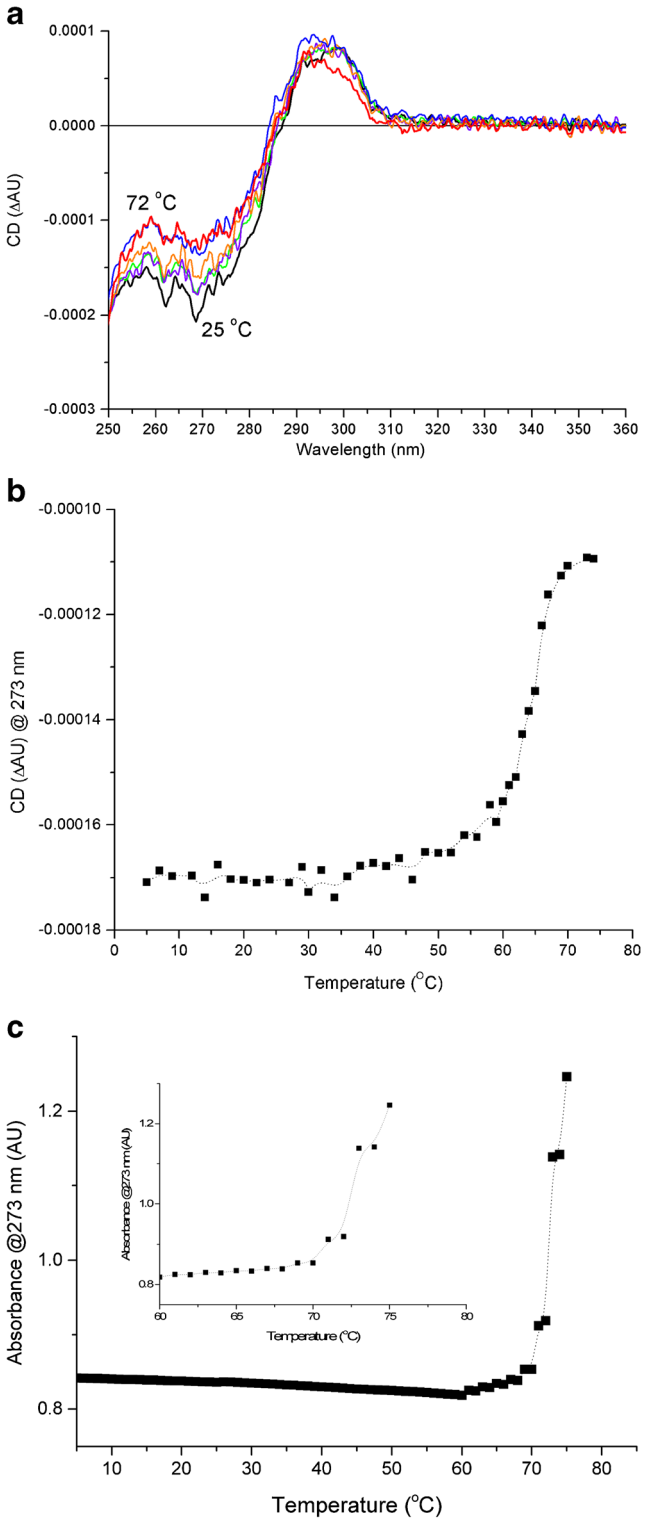


**Fig. 3** **a** Near-UV CD spectra at 25 °C (*black*) and at 72 °C (*red*) (IgG at 1 mg/mL in CBS, l=0.5 cm). Other spectra at intermediate temperatures are shown in between: 60 °C (*green*), 62 °C (*violet*), 64 °C (*orange*) and 65 °C (*blue*). **b** Near-UV CD (ΔAU) changes upon temperature incubation followed at 273 nm. **c** Absorbance at 273 nm recorded by the instrument during data acquisition. An increase in the absorbance value is indicative of an increase in scattering linked to aggregation

fluorescence signal decreases until 60 °C and then increases (Fig. 4a). This could be due to the removal, upon unfolding, of the quenching due to groups that are close to the Trp in the folded structure [25, 32]. Because of the presence of two shoulders in the fluorescence spectrum, indicative of the presence of two tryptophan populations experiencing different environments, to follow the shift in $\lambda_{max}$, we have expressed the changes as the ratio between the intensity at 330 and 350 nm (Fig. 4c). The rationale behind this choice is that the ratio between these two intensities is proportional to the relative fraction of "more exposed tryptophans" (max at higher wavelengths) versus "more buried tryptophans" (max at lower wavelengths) at the stated temperature. The first changes start to occur between 60 and 65 °C, as in the case of the near-UV CD spectra, with a shift in the $\lambda_{max}$ position that indicates an overall increase in the polarity of the environment of the tryptophan residues (Fig. 4b).

Overall, these results suggest that the first transition, occurring before 65 °C, involves a loss of rigidity in the phenylalanine and tyrosine regions and a change in the polarity of the environment of the tryptophans. Depending on the IgG concentration, irreversible aggregation occurs around the temperature of the onset of the second transition.

*Changes in the aggregation state upon thermal denaturation* One of the drawbacks when using multiple techniques is the need to dilute the sample to be in the technique dynamic range. So, while the sample was forming irreversible, gel-like aggregates when the thermal stability was measured at 1 mg/mL or higher, the sample used for fluorescence measurements (0.1 mg/mL) does not form visible aggregates up to 75 °C. The concentration dependence of the onset of the aggregation is expected, because aggregation, being a higher-order process, depends upon protein concentration.

To correlate the changes, observed with the previous techniques, with changes in the association state, we have measured the concentration dependence of the aggregation temperature ($T_{agg}$) by DLS at 1 and 81 mg/mL.

As expected, the higher the concentration, the earlier the onset of the formation of soluble aggregates, $T_{agg}$ (Fig. 5—around 65 °C for the 81-mg/mL solution and 72 °C for the solution at 1 mg/mL) and, on average, the greater the relative size of the aggregates at the same temperature (ESM Fig. S7). The correlograms were analysed both with a single exponential function ($Z_{ave}$) and with a multimodal distribution, but no differences were observed by using the two methods (ESM Fig. S8).

Upon further temperature increase, the sample forms insoluble gel-like aggregates. This temperature can be deduced

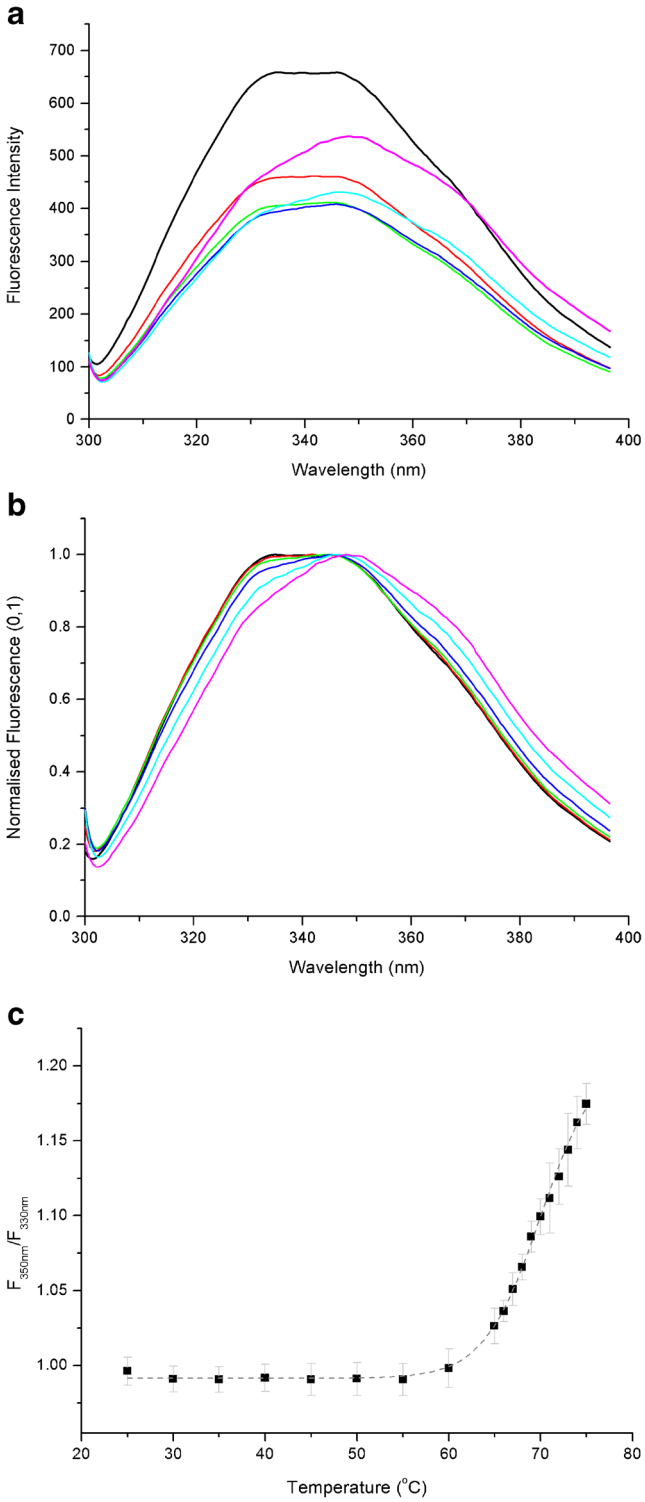


**Fig. 4** Variation of the **a** intrinsic fluorescence intensity and **b** normalised intensity with the temperature (IgG at 0.1 mg/mL in CBS). $T$=25 °C (*black*), $T$=50 °C (*red*), $T$=60 °C (*green*), $T$=65 °C (*blue*), $T$=70 °C (*cyan*), and $T$=75 °C (*magenta*). **c** Thermal denaturation followed by the intensity ratio $F_{350\ nm}/F_{330\ nm}$

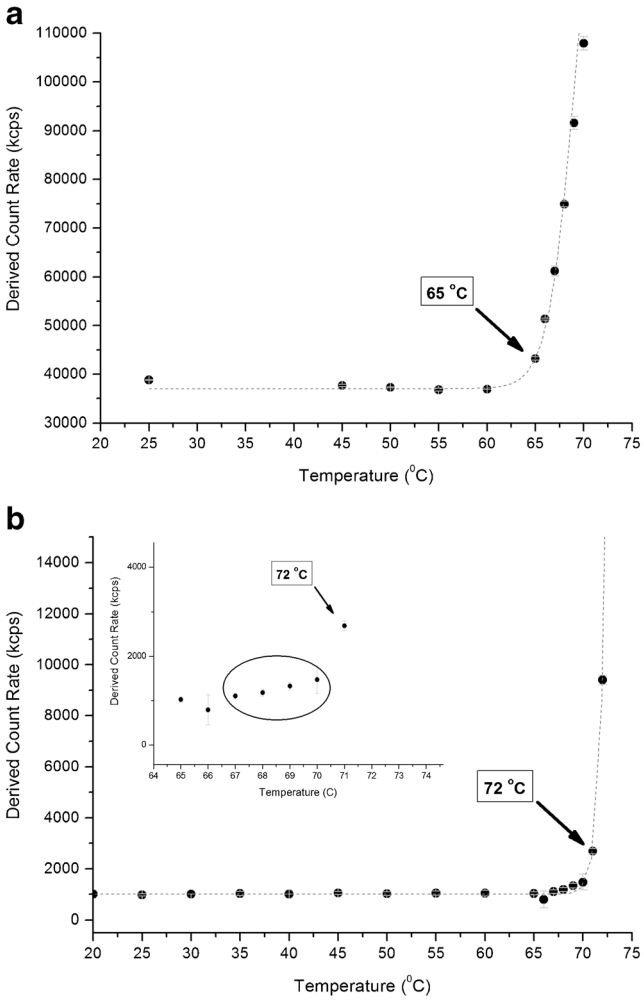


**Fig. 5** DLS measurements reporting the variation in the scattered intensity with increasing temperature of **a** 81 mg/mL and **b** 1 mg/mL of IgG solutions in CBS

from the sudden change in the correlograms between 72 and 73 °C (ESM Fig. S9) and by the sudden increase of polydispersity index (Fig. 6). It should be noted that the gelation temperature (formation of irreversible and insoluble aggregates) is the same for both the concentrations and that it occurs at a temperature close to the second transition temperature observed by DSC.

The PdI increases with temperature for both the samples, but to a different extent (Fig. 6). The 1-mg/mL solution remains relatively monodisperse (PdI<0.2 with a good standard deviation between replicates) below 65 °C. Above this temperature, there is the formation of higher molecular weight species up to the onset of the irreversible aggregation at 72 °C. The 81-mg/mL solution presents, instead, a steady increase in the PdI at 65 and 67 °C, where the PdI reaches a plateau until the onset of the irreversible aggregation at 72 °C.

*Structure of the irreversible aggregate* At around 72–73 °C, the IgG undergoes irreversible aggregation, forming a white

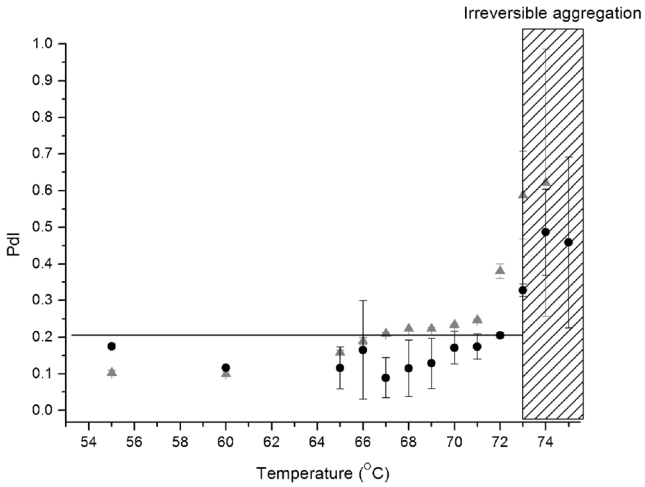


**Fig. 6** PdI changes with increasing temperature. IgG solutions in CBS at 1 mg/mL (*black*) and 81 mg/mL (*grey*)

gel. The "gel-solid" spectra were determined by subtracting, from the spectra of the gel as a whole, the contribution of the soluble species (see "Experimental" section).

The FTIR spectra of the gel present a shift in the peak position of the amide I band from 1,636 toward 1,623 $cm^{-1}$, a value that is indicative of the formation of intermolecular β-sheet structures (Fig. 7).

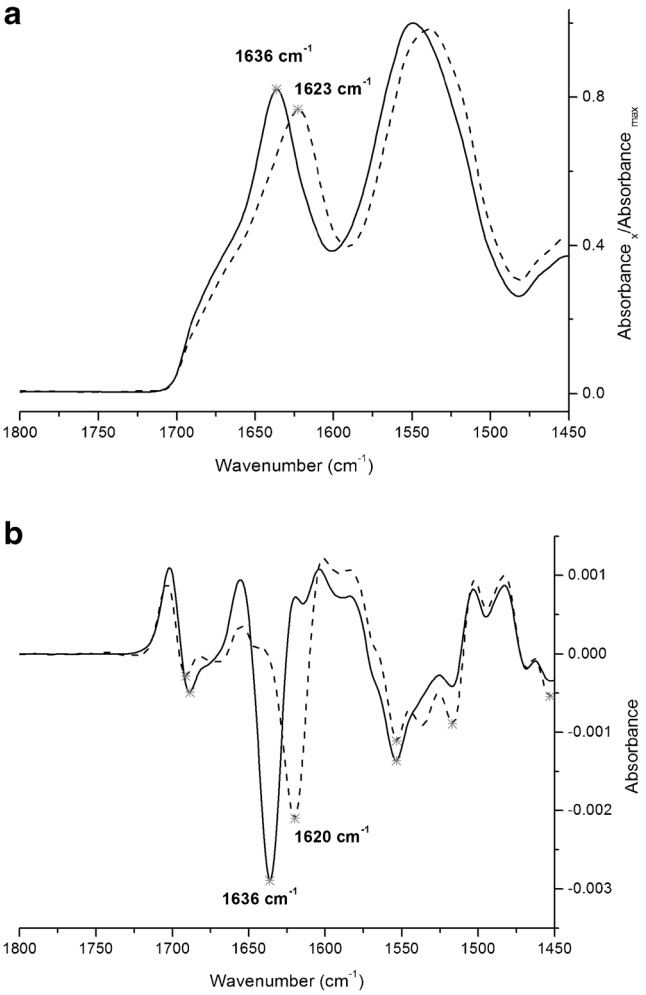


**Fig. 7** FTIR-ATR spectra (normalised) (**a**) and second derivative spectra (**b**) for the IgG solution and the gel obtained after melt

## Conclusions

Thermal denaturation of multi-domain proteins often results in the formation of irreversible aggregates, which are likely to proceed from partially unfolded conformations with hydrophobic patches exposed in a regular array [11]. The increase in temperature affects the aggregation process in different ways. First of all, it determines an increase in the frequency of the collisions of these partially unfolded, aggregation-prone intermediates, increasing the likelihood of the association events. Moreover, the strength of the hydrophobic interactions, which are mainly responsible for aggregate formation, increases with temperature [5]. Finally, protein flexibility is enhanced, and this translates into an increase in the frequency of breakage and reformation of hydrogen bonds. This can lead to the formation of intermolecular bonds instead of intramolecular ones, leading to aggregation [33].

Our data suggests that, for this particular IgG, aggregation occurs between intermediates that have partially lost their tertiary structure but retain their secondary structure. In particular, the DSC thermogram shows the presence of two transitions due, very likely, to the unfolding of different domains. Of these two transitions, only the second one leads to irreversible aggregation, whereas the first one leads to the formation of soluble oligomers, as demonstrated by the DLS experiments.

The formation of soluble oligomers follows the partial unfolding of the IgG tertiary structure and depends on the amount of unfolded species in solution (the higher the protein concentration, the earlier the onset of the formation of the soluble oligomers).

The irreversible aggregation process (that is, the formation of intermolecular β-sheet structure and gelation), instead, depends on both the unfolding of the other IgG domains (second transition observed in the DSC thermogram) and on the presence of a critical concentration of soluble oligomers which seems to act as nuclei for the process. This would explain why the gelation temperature is the same for the 1- and 81-mg/mL (in both cases, there is a minimum population of oligomers in solution at the onset of the second transition), but no irreversible precipitation was observed for the 0.1-mg/mL sample (Table 2). In this case, though the shift in the $\lambda_{max}$ indicates an increase of Trp exposure to the solvent, and therefore unfolding, no gelation occurs at 72 °C. This suggests that, at the concentrations used for fluorescence experiments, the critical concentration of nuclei is not reached.

**Table 2** Summary of the techniques, experimental conditions and results

| Technique | [IgG] (mg/mL) | Notes | Aggregation |
|---|---|---|---|
| DSC | 81 | ~63 °C (onset); ~76 °C $T_m$ | Yes |
| Far-UV CD | 1 | No changes until onset of aggregation (~75 °C) | Yes |
| FTIR-ATR | 81 | No changes until onset of aggregation (~70–75 °C) | Yes |
| Near-UV CD | 1 | After 60 °C: small changes in Trp, loss of rigidity in the Phe and Tyr regions | Yes |
| Fluorescence | 0.1 | Changes after 60 °C | No |
| DLS | 1 and 81 | $T_{agg}$: concentration dependent; $T_{gel}$ concentration independent | Yes |

At the onset of the second transition, leading to irreversible aggregation, the changes in the near-UV CD region are completed. These changes involve mainly the Phe and Tyr regions, while in the Trp regions, small changes and no loss of signal can be seen. Therefore, the formation of soluble oligomers follows the partial "loosening" of the tertiary structure. In this process, the tryptophans do not experience a dramatic change in the rigidity of their environment (e.g. unfolding), and upon further heating, they are locked in a partially folded conformation in the aggregate. This can determine a different Trp environment from the native state and would explain the differences observed in the Trp region of the near-UV CD spectra where a change in the spectrum, but not a decrease of signal is observed. This is also consistent with the increase in $\lambda_{max}$ in the fluorescence upon temperature increase.

Overall, these data suggests that the unfolding of the first domain results in the formation of soluble oligomers, whereas the unfolding of the second domain causes the locking of these preformed nuclei in intermolecularly bonded β-sheet irreversible aggregates. Therefore, we can describe the unfolding process in the following way (where the subscripts 1 and 2 refer to two different domains):

$$\begin{array}{ll} N_1N_2 \Leftrightarrow & U_1N_2 \\ nU_1N_2 \Leftrightarrow (U_1N_2)_{n\ (soluble)} & \rightarrow (U_1U_2)_{n\ (insoluble)} \text{ or } (U_1N_2)_{n\ (insoluble)} \end{array}$$

The unfolding of the first domain ($N_1 \rightarrow U_1$) determines the exposure of hydrophobic patches that can interact intermolecularly in a native-like way (no changes in far-UV CD and FTIR—$nU_1N_2 \rightarrow (U_1N_2)_n$).

When the concentration of these intermediates is high enough, a further increase of temperature could cause the unfolding of the other domain ($N_2 \rightarrow U_2$). Though we cannot infer from our data if this last step occurs or not, our experiments suggest that the irreversible aggregation occurs through the association of the preformed nuclei ($(U_1U_2)_{n\ (insoluble)}$ or $(U_1N_2)_{n\ (insoluble)}$), leading to the formation of intermolecular β-sheet aggregates.

Therefore, the destabilisation of the soluble oligomers can be a strategy to increase the stability of this IgG solution.

**Acknowledgments** We thank the UK Department of Business Innovation and Skills for funding the work and GSK for the immunoglobulin sample. We thank Alex Knight, Anna Hills, Adrian Horgan, Paulina Rakowska and Max Ryadnov for reviewing the manuscript and Michael Molloy for sourcing the sample.

## References

1. Wang W, Singh S, Zeng DL, King K, Nema S (2007) Antibody structure, instability, and formulation. J Pharm Sci 96(1):1–26
2. Samra HS, He F (2012) Advancements in high throughput biophysical technologies: applications for characterization and screening during early formulation development of monoclonal antibodies. Mol Pharm 9:696–707
3. Frokjaer S, Otzen DE (2005) Protein drug stability: a formulation challenge. Nat Rev Drug Discov 4(4):298–306
4. Wang W (2005) Protein aggregation and its inhibition in biopharmaceutics. Int J Pharm 289(1–2):1–30
5. Arakawa T, Philo JS, Ejima D, Tsumoto K, Arisaka F (2006) Aggregation analysis of therapeutic proteins, part 1. Bioprocess Int 4(10):32–42
6. Arakawa T, Philo JS, Ejima D, Tsumoto K, Arisaka F (2007) Aggregation analysis of therapeutic proteins, part 2. BioProcess Int 5(4):36–47
7. Hermeling S, Crommelin DJ, Schellekens H, Jiskoot W (2004) Structure-immunogenicity relationships of therapeutic proteins. Pharm Res 21(6):897–903
8. Chirino AJ, Ary ML, Marshall SA (2004) Minimizing the immunogenicity of protein therapeutics. Drug Discov Today 9(2):82–90
9. Rosenberg AS (2006) Effects of protein aggregates: an immunologic perspective. AAPS J 8(3):E501–507
10. Wang W, Singh SK, Li N, Toler MR, King KR, Nema S (2012) Immunogenicity of protein aggregates—concerns and realities. Int J Pharm 431:1–11
11. Roberts CJ (2006) Nonnative protein aggregation. misbehaving proteins, protein (mis) folding, aggregation, and stability. Murphy, Regina; Tsai, Amos (Eds)
12. Kendrick BS, Li T, Chang BS (2002) Physical stabilization of proteins in aqueous solution. Pharm Biotechnol 13:61–84
13. Garber E, Demarest SJ (2007) A broad range of Fab stabilities within a host of therapeutic IgGs. Biochem Biophys Res Commun 355(3): 751–757
14. Vermeer AW, Norde W, van Amerongen A (2000) The unfolding/denaturation of immunogammaglobulin of isotype 2b and its F(ab) and F(c) fragments. Biophys J 79(4):2150–2154
15. Vermeer AW, Norde W (2000) The thermal stability of immunoglobulin: unfolding and aggregation of a multi-domain protein. Biophys J 78(1):394–404

16. Heads JT, Adams R, D'Hooghe LE, Page MJT, Humphreys DP, Popplewell AG, Lawson AD, Henry AJ (2012) Relative stabilities of OgG1 and IgG4 Fab domains: influence of the light-heavy interchain disulphide bond architecture. Protein Sci 21:1315–1322
17. Ionescu RM, Vlasak J, Colleen P, Kirchmeier M (2008) Contribution of variable domains to the stability of humanized IgG1 monoclonal antibodies. J Pharm Sci 97(4):1414–1426
18. Lee JC (2000) Biopharmaceutical formulation. Curr Opin Biotechnol 11(1):81–84
19. Cleland JL, Powell MF, Shire SJ (1993) The development of stable protein formulations: a close look at protein aggregation, deamidation, and oxidation. Crit Rev Ther Drug Carrier Syst 10(4): 307–377
20. Chang BS, Hershenson S (2002) Practical approaches to protein formulation development. Pharm Biotechnol 13:1–25
21. Baynes BM, Trout BL (2004) Rational design of solution additives for the prevention of protein aggregation. Biophys J 87(3):1631–1639
22. Cooper A, Johnson CM (1994) Differential scanning calorimetry. Methods Mol Biol 22:125–136
23. Wilcox A, Krishnamurthy R (2006) Application of spectroscopic and calorimetric techniques in protein formulation development. misbehaving proteins, protein (mis) folding, aggregation, and stability. Murphy, Regina; Tsai, Amos (Eds)
24. Weichel M, Bassarab S, Garidel P (2008) Probing thermal stability of MAbs by intrinsic tryptophan fluorescence. BioProcess Int 6(6):42–52
25. Murphy RM, Lee CC (2006) Laser light scattering as an indispensable tool for probing protein aggregation. Misbehaving proteins, protein (mis) folding, aggregation, and stability. Murphy, Regina; Tsai, Amos (Eds)
26. Demeule B, Lawrence MJ, Drake AF, Gurny R, Arvinte T (2007) Characterization of protein aggregation: the case of a therapeutic immunoglobulin. Biochim Biophys Acta 1774(1):146–153
27. Philo JS (2006) Is any measurement method optimal for all aggregate sizes and types? Aaps J 8(3):E564–571
28. Daugherty AL, Mrsny RJ (2006) Formulation and delivery issues for monoclonal antibody therapeutics. Adv Drug Deliv Rev 58(5–6): 686–706
29. Dousseau FTM, Pezolet M (1989) On the spectral subtraction of water from the FTIR spectra of aqueous solutions of proteins. Appl Spectrosc 43(3):538–542
30. BS3406-8, ISO13321 (1997) Determination of particle size distribution—part 8: photon correlation spectroscopy. BS
31. Hawe A, Friess W, Sutter M, Jiskoot W (2008) Online fluorescent dye detection method for the characterization of immunoglobulin G aggregation by size exclusion chromatography and asymmetrical flow field flow fractionation. Anal Biochem 378(2):115–122
32. Ladokhin AS (2000) Fluorescence spectroscopy in peptides and protein analysis. Encyclopedia of analytical chemistry. RA Meyers (Ed.):5762-5779
33. McCarthy DA, Drake AF (1989) Spectroscopic studies on IgG aggregate formation. Mol Immunol 26(9):875–881